Hindawi Publishing Corporation
Journal of Nanomaterials
Volume 2013, Article ID 864374, 11 pages
http://dx.doi.org/10.1155/2013/864374

Research Article

Fabrication of Novel Biodegradable α-Tricalcium Phosphate Cement Set by Chelating Capability of Inositol Phosphate and Its Biocompatibility

Toshiisa Konishi,[1,2] Minori Mizumoto,[2] Michiyo Honda,[2] Yukiko Horiguchi,[3] Kazuya Oribe,[3] Hikaru Morisue,[4] Ken Ishii,[2,4] Yoshiaki Toyama,[4] Morio Matsumoto,[2,4] and Mamoru Aizawa[1,2]

[1] *Department of Applied Chemistry, School of Science and Technology, Meiji University, 1-1-1 Higashimita, Tama-ku, Kawasaki 214-8571, Japan*
[2] *Kanagawa Academy of Science and Technology (KAST), KSP East 404, 3-2-1 Sakado, Takatsu-ku, Kawasaki 213-0012, Japan*
[3] *Showa Ika Kohgyo Co., Ltd., 8-7 Hanei-nishimachi, Toyohashi 441-8026, Japan*
[4] *Department of Orthopaedic Surgery, School of Medicine, Keio University, 35 Shinanomachi, Shinjuku-ku, Tokyo 160-8582, Japan*

Correspondence should be addressed to Toshiisa Konishi; ap-konishi@newkast.or.jp

Received 8 April 2013; Accepted 8 May 2013

Academic Editor: Eng San Thian

Biodegradable α-tricalcium phosphate (α-TCP) cement based on the chelate-setting mechanism of inositol phosphate (IP6) was developed. This paper examined the effect of the milling time of α-TCP powder on the material properties of the cement. In addition, biocompatibility of the result cement *in vitro* using osteoblasts and *in vivo* using rabbit models will be studied as well. The α-TCP powders were ballmilled using ZrO_2 beads in pure water for various durations up to 270 minutes, with a single-phase α-TCP obtained at ballmilling for 120 minutes. The resulting cement was mostly composed of α-TCP phase, and the compressive strength of the cement was 8.5 ± 1.1 MPa, which suggested that the cements set with keeping the crystallite phase of starting cement powder. The cell-culture test indicated that the resulting cements were biocompatible materials. *In vivo* studies showed that the newly formed bones increased with milling time at a slight distance from the cement specimens and grew mature at 24 weeks, and the surface of the cement was resorbed by tartrate-resistant acid phosphatase-(TRAP-)positive osteoclast-like cells until 24 weeks of implantation. The present α-TCP cement is promising for application as a novel paste-like artificial bone with biodegradability and osteoconductivity.

1. Introduction

Hydroxyapatite ($Ca_{10}(PO_4)_6(OH)_2$; HAp) has been used as bioceramics for bone grafting due to its biocompatibility and osteoconductivity. HAp is used clinically in the following forms: granule, dense ceramics, porous ceramics, and cement (paste-like artificial bone). In particular, the cement, that is, calcium-phosphate cement (CPC), has an advantage in that desired shape can be easily formed during surgery operation and has therefore received much attention [1–4].

CPCs generally consist of a mixture of a calcium-phosphate powder and an aqueous solution, and they are classified into two types. One type is based on hydrolysis of α-tricalcium phosphate (α-$Ca_3(PO_4)_2$; α-TCP) put forward by Monma and Kanazawa [5]. The other type is based on acid-base reaction of tetracalcium phosphate ($Ca_4O(PO_4)_2$; TTCP) and acidic dicalcium phosphate dihydrate ($CaHPO_4 \cdot 2H_2O$; DCPD) put forward by Brown and Chow [6]. Both CPCs are set by precipitation of calcium-deficient HAp (CDHA) or HAp; thus, they are stable in a host body for a long time [7].

We have developed a novel CPC using inositol phosphate ($C_6H_6(OPO_3H_2)_6$; IP6) as a chelating agent [8–11]. IP6 is found in wheat, rice, corn, and soybean [12], and it has a strong chelating capability to calcium ions, similar to chelating compounds such as ethylenediaminetetraacetic

acid (EDTA) [13]. The newly developed cement was created by mixing HAp powders that were surface modified with IP6 and suitable mixing solutions, and it could set by the chelate bonding of IP6. In addition, this cement showed excellent biocompatibility both *in vitro* and *in vivo* [11]. Meanwhile, we have previously developed biodegradable cement consisting of a single-phase β-TCP based on the chelate-setting mechanism of IP6, which was biodegradable and osteoconductive *in vivo* using rabbit models [14–16].

The order in relative dissolution of the calcium phosphates is α-TCP > β-TCP > HAp [17, 18]. Thereby, more soluble and reactive α-TCP than β-TCP is used mainly as a fine powder in hydraulic cement [5, 17, 18], and it is impossible to fabricate a single-phase α-TCP cement using neutral liquid component; that is, cement set with keeping a crystallite phase of starting reactant. Yamada et al. [19] have reported a histological and histomorphometrical study of porous β-TCP and α-TCP blocks as bone graft materials for augmenting alveolar ridges, in which the α-TCP block notably started degrading after 4 weeks, whereas degradation of β-TCP blocks had just begun at that time and scarcely progressed after 8 weeks. These results suggest that resorption of α-TCP is faster than that of β-TCP. Therefore, it is hypothesized that a novel biodegradable cement using more soluble α-TCP powder compared with β-TCP powder can develop on the basis of the chelate-setting mechanism of IP6, which will be a more biodegradable cement than β-TCP cement.

Our final goal is to develop injectable α-TCP cement with suitable mechanical property, biodegradability, and biocompatibility, on the basis of the chelate-setting mechanism of IP6. In this paper, the α-TCP cement based on chelate-setting mechanism of IP6 was fabricated. The α-TCP powders for cement fabrication were prepared by grinding and then modifying their surface with IP6, and mechanical property of the α-TCP cement was investigated in order to obtain the basic findings for development of injectable CPC. Moreover, biocompatibility of the α-TCP cement was examined *in vitro* using osteoblasts model and *in vivo* using rabbit models.

2. Materials and Methods

2.1. Preparation of the Ball-Milled α-TCP Powders and Their Surface Modification with IP6. The IP6 (50 mass % phytic acid, Wako Pure Chemical Industries, Ltd., Japan) solution was prepared with a concentration of 1000 ppm and was adjusted to pH 7.3 using an aqueous solution of NaOH (0.1 mol·dm^{-3}). 10 grams of commercially available α-TCP powder (α-TCP-A, Taihei Chemical Industrial Co., Ltd., Japan) were ground using a planetary mill (Pulverisette 6, Fritsch, Germany) for 30, 60, 90, 120, 180, 240, and 270 minutes at a rotation rate of 300 rpm in a ZrO_2 pot with fifty 10 mm diameter ZrO_2 beads under wet conditions (40 cm^3 of pure water). After ball-milling, the slurry mixtures were filtrated, and freeze-dried for 24 h to prepare ball-milled α-TCP powder without surface modification with IP6. To prepare the IP6 surface modified α-TCP powder, the filter cake obtained was added into the IP6 solution (400 cm^3), stirred at 400 rpm for 24 h, filtrated, and freeze dried for 24 h.

Hereafter, samples are denoted according to the milling time; for example, the α-TCP powder ball-milled for 120 minutes is denoted as "α-TCP120", and the α-TCP120 powder surface modified with IP6 is denoted as "IP6-α-TCP120". The as-received α-TCP-A powder is denoted as "α-TCP0".

2.2. Characterization of the Prepared α-TCP Powders. X-ray diffraction (XRD; Ultima IV, Rigaku, Japan) analysis of the powders was conducted using a CuKα radiation source. Data were collected in the range of $2\theta = 25 - 40^\circ$ with a step size of 0.02° and counting time of 1.2 s/step. The crystal phase was identified with respect to the JCPDS reference patterns for α-TCP (#09-0348) and HAp (#09-0432). The HAp content in the α-TCP powders with and without IP6 surface modification was calculated using the typical peaks of α-TCP ($2\theta = 30.75^\circ$) and HAp ($2\theta = 31.77^\circ$) by (1) as follows:

$$\text{HAp content (\%)} = \frac{\left(I_{\text{HAp}(t)}\right)}{\left(I_{\alpha\text{-TCP}(t)} + I_{\text{HAp}(t)}\right)} \times 100, \quad (1)$$

where $I_{\alpha\text{-TCP}(t)}$ and $I_{\text{HAp}(t)}$ are the XRD intensities of the α-TCP ($2\theta = 30.75^\circ$) and HAp ($2\theta = 31.77^\circ$) in the ball-milled powder for t min ($t = 0 - 270$), respectively. The crystallite size of the ball-milled α-TCP powders was calculated using Scherrer's equation:

$$\text{Crystallite size (nm)} = \frac{K\lambda}{\beta \cos\theta}, \quad (2)$$

where K is the shape coefficient ($K = 0.9$), λ is the wavelength ($\lambda = 0.15405$ nm), and β is the half width at $2\theta = 30.75^\circ$.

The specific surface area and median particle size of the ball-milled α-TCP powders were measured with a surface area analyzer (Flowsorb III, Shimadzu, Japan) and a laser particle size analyzer (LA-300, Horiba, Japan), respectively. The particle morphology of the ball-milled α-TCP sputter coated with Au was observed with a scanning electron microscope (SEM; VE-9800, Keyence, Japan) at an accelerating voltage of 10 kV.

Dissolution of Ca^{2+} ions released from the ball-milled α-TCP powder with and without IP6 surface modification was measured using ion-selective potentiometry (F-73, Horiba, Japan). Twenty-five milligrams of each α-TCP powder were added to 0.2 dm^3 of 0.05 mol·dm^{-3} tris (hydroxymethyl) aminomethane hydrochloric acid (Tris-HCl) buffer at pH 7.3 and 25 ± 3°C with stirring at 430 rpm. The concentration of free Ca^{2+} ions in the solution was measured as a function of time up to 180 minutes.

2.3. Fabrication of the α-TCP Cement Specimens and Their Material Properties. Cement specimens were fabricated by mixing 0.25 g of prepared α-TCP powder with and without surface modification with IP6 and pure water at powder/liquid (P/L) ratio of 1/0.40 [g/cm^3], and packing into a 5 mm diameter cylindrical stainless mold. The resulting cement specimens (5 mm in diameter, 7 mm in height) were kept at room temperature for 24 h.

The compressive strength of the cement specimens was measured using a universal testing machine (Autograph

AGS-X, Shimadzu, Japan) with a 5 kN load cell at a crosshead speed of 500 μm·min^{-1}. XRD patterns of the cement after the compressive strength testing were measured to determine the HAp content after setting for 24 h, and the HAp content in the cement specimen was also calculated by (1). The microstructure of the fracture cement sputter coated with Au was observed with SEM at an accelerating voltage of 10 kV. The bulk density of the cylindrical cement specimens was calculated by measuring the diameter, height, and weight of the cement. The relative density of the cement specimen was calculated from the bulk density divided by the theoretical density of α-TCP/HAp, which was calculated by (3) as follows:

$$\begin{aligned}\text{Theoretical density of } \alpha\text{-TCP/HAp } \left(\text{g/cm}^3\right) \\ = \frac{2.86 \times \left(100 - \text{HAp content } (\%)\right)}{100} \\ + \frac{3.16 \times \left(\text{HAp content } (\%)\right)}{100},\end{aligned} \tag{3}$$

where 2.86 and 3.16 [g/cm^3] are theoretical density of the α-TCP and HAp, respectively.

2.4. In Vitro Evaluation of the α-TCP Cement Specimens. In order to evaluate the biocompatibility of the cement specimens, we have compared cell proliferation between polystyrene plate (control) and cement specimens (both α-TCP120 and IP6-α-TCP120). The IP6-α-TCP120 cement with the highest compressive strength and the lowest HAp contents was selected, which would be expected as the most biodegradable material.

The cement specimens for *in vitro* evaluation were prepared by mixing the α-TCP powder and pure water at P/L ratio of 1/0.4 [g/cm^3], and packing into a cylindrical stainless mold. The resulting cement specimens (5 mm in diameter, 7 mm in height) were kept at room temperature under atmospheric conditions for 24 h, and they were sterilized with ethylene oxide gas (EOG).

Osteoblast-like cells (MC3T3-E1) were seeded into 12 well tissue culture plates at a density of 6×10^4 cells/well and precultured for 1 day. The cement specimens were then set on a membrane of Transwell kit (Corning, USA) to culture the cells in a humidified 5% CO_2 balanced-air incubator at 37°C. The number of proliferated cells was counted after culturing for 1, 2, and 4 days.

2.5. In Vivo Evaluation of the α-TCP Cement Specimens. Based on *in vitro* cell proliferation assay, biodegradability and biocompatibility of the IP6-α-TCP120 cement specimens *in vivo* were evaluated.

In vivo studies of the IP6-α-TCP120 cement specimens were performed using 16-week-old male rabbits (average weight: 3 kg) according to the guidelines of the laboratory animal center at Keio University. The cement specimens for *in vivo* evaluation were prepared in the same manner as described in Section 2.4. The dimensions of the resulting cement specimens were 4 mm in diameter and 7 mm in height. The cement specimens were sterilized with EOG.

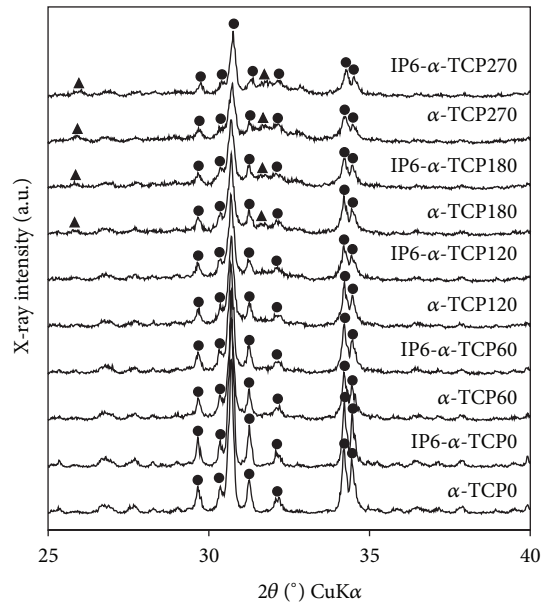

Figure 1: XRD patterns of the prepared α-TCP powders with and without IP6 surface modification. Closed circles indicated typical α-TCP peaks, and closed triangles indicated typical HAp peaks. The single-phase α-TCP was maintained up to 120 minutes of milling, and the α-TCP powders over 120 minutes of milling were composed of both α-TCP and HAp phases.

A cylindrical defect (4.4 mm diameter) was drilled in the epiphysis of a rabbit's tibia. The cement specimen was implanted into the defect for 4, 8, and 24 weeks. At appropriate period, the rabbit was sacrificed using sodium pentobarbital and the tibia was removed. Decalcified and undecalcified sections were then prepared for histological evaluation. The decalcified sections were stained with tartrate-resistant acid phosphatase (TRAP) and the undecalcified sections were stained with hematoxylin and eosin (HE). The histological sections were observed with an upright microscope (BX41, Olympus, Japan).

2.6. Statistical Analysis. A t-test was used to determine whether any significant differences existed between the mean values of the experimental groups. A difference between groups was considered to be significant at $P < 0.05$.

3. Results

3.1. Characterization of the Prepared α-TCP Powders. Typical XRD patterns, crystallite size, and HAp content of the prepared α-TCP powders were shown in Figures 1 and 2, respectively. The XRD patterns of the as-received α-TCP powder (α-TCP0) and the IP6 surface modified powder (IP6-α-TCP0) showed that α-TCP had a single phase with high crystallinity. The XRD patterns of the α-TCP powders ball milled up to 120 minutes and their surface-modified powders showed mostly α-TCP phase.

In Figure 2, the crystallite size of the prepared α-TCP powders with and without IP6 surface modification

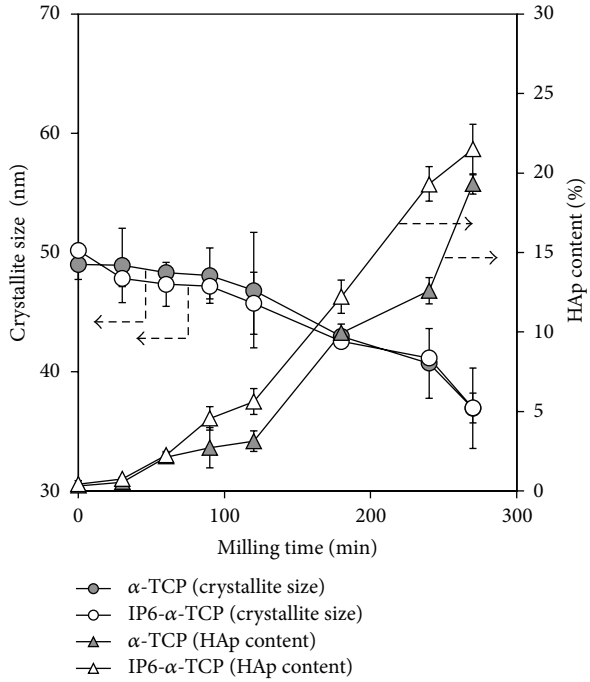

Figure 2: Crystallite size and HAp content of the prepared α-TCP powders with and without IP6 surface modification as a function of milling time. Error bars indicated standard error of the mean ($n = 3$). The crystallite size of the prepared α-TCP powders with and without IP6 surface modification decreased with milling time, and HAp contents of the prepared α-TCP powders with and without IP6 surface modification increased with milling time.

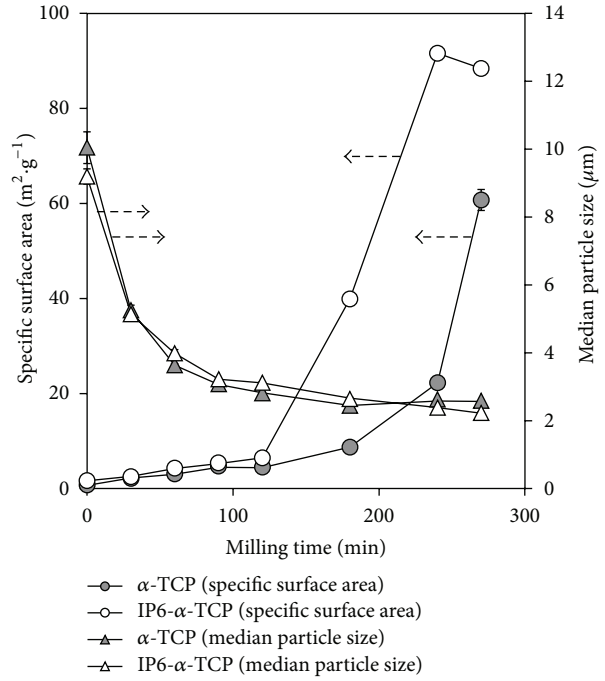

Figure 3: Specific surface area and median particle size of the prepared α-TCP powders with and without surface modification as a function of milling time. Error bars indicated standard error of the mean ($n = 3$). The specific surface area of the α-TCP powders up to 120 minutes of ball milling did not change before and after IP6 surface modification; however, that of the IP6 surface modified α-TCP powders over 180 minutes of milling was higher than that of the α-TCP powders before IP6 surface modification. Median particle size of the prepared α-TCP powders decreased with increasing milling time.

decreased with milling time, and the prepared α-TCP powders were composed of nanosized α-TCP crystals less than 50 nm. Although the α-TCP180 and IP6-α-TCP180 powders were mostly composed of α-TCP phase, small amount of HAp phase was contained: 9.9 ± 0.6% for the α-TCP180 and 12.2 ± 1.1% for the IP6-α-TCP180. The HAp contents in the IP6 surface modified α-TCP powders over 90 minutes of ball milling were more than those of the α-TCP powders without IP6 surface modification, which suggested that the α-TCP powders without IP6 surface modification were hydrolyzed during IP6 surface modification.

Specific surface area and median particle size of the prepared α-TCP powders were shown in Figure 3. Specific surface area of the α-TCP powders up to 120 minutes of ball milling did not change before and after IP6 surface modification; however, that of the IP6 surface modified α-TCP powders over 180 minutes of milling was higher than that of the α-TCP powders before IP6 surface modification. The results corresponded to the increase in HAp contents of IP6 surface modified α-TCP powders over 180 minutes of milling in Figure 2. Median particle size of the prepared α-TCP powders decreased with increasing milling time, and that of the prepared α-TCP powders with and without IP6 surface modification did not change. Although the median particle size of IP6-α-TCP0 powder was about 9.2 ± 0.2 μm, that of IP6-α-TCP120 powder composed of a single phase α-TCP decreased to approximately 3.1 ± 0.04 μm.

Figure 4 showed particle morphology of the prepared α-TCP powders. In Figures 4(a) and 4(b), the α-TCP0 and IP6-α-TCP0 powders were tens of microns of grains; however, the particle size of the α-TCP powders decreased with increasing milling time (Figures 4(c)–4(h)). The results were consistent with the decrease in median particle size and crystallite size of the prepared α-TCP powders. The α-TCP180 and IP6-α-TCP180 powders were composed of small particles and aggregates as indicated by arrows (Figures 4(g) and 4(h)), and in highly magnification images these aggregates were composed of needle-shaped crystals (data not shown). In addition, no obvious difference in the particle morphology with and without IP6 surface modification was observed.

The dissolution of Ca^{2+} ions from the prepared α-TCP powders was shown as a function of time up to 180 minutes (Figure 5). Dissolution of the IP6-α-TCP powders was lower than that of α-TCP powders without IP6 surface modification, whereas dissolution of the α-TCP powders with and without IP6 surface modification increased with milling time.

3.2. Evaluation of the α-TCP Cement Specimens. XRD patterns of the cement specimens, after setting for 24 h, fabricated from the α-TCP powders with and without IP6 surface

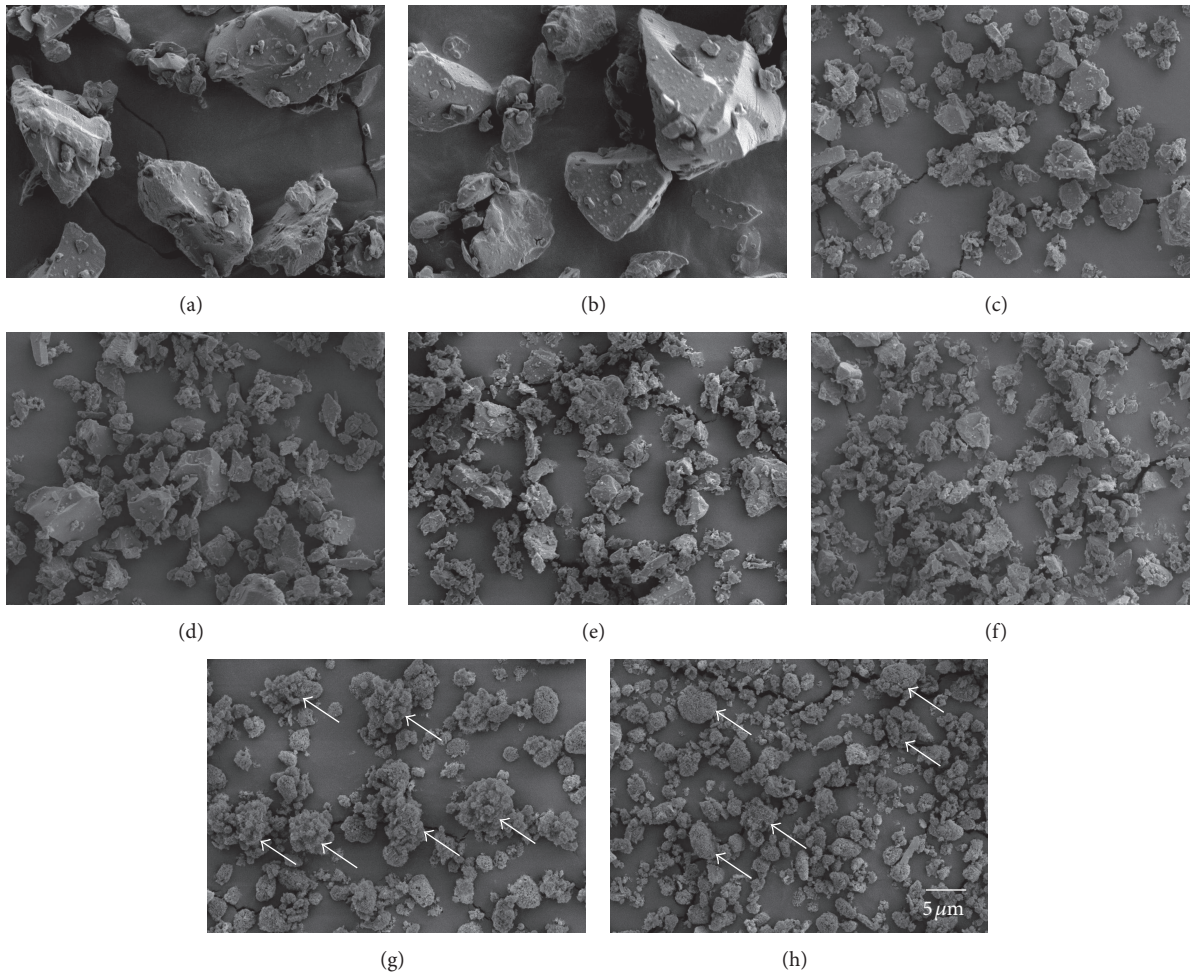

Figure 4: Particle morphology of the prepared α-TCP powders: (a) α-TCP0, (b) IP6-α-TCP0, (c) α-TCP60, (d) IP6-α-TCP60, (e) α-TCP120, (f) IP6-α-TCP120, (g) α-TCP180, and (h) IP6-α-TCP180. In (a) and (b), the α-TCP0 and IP6-α-TCP0 powders were tens of microns of grains; however, the particle size of the α-TCP powders decreased with increasing milling time ((c)–(h)). The α-TCP180 and IP6-α-TCP180 powders were composed of small particles and aggregates as indicated by arrows ((g) and (h)).

modification at the P/L = 1/0.40 [g/cm^3] were measured, and HAp content of those cement specimens was calculated using (1) (Figure 6). The XRD patterns of α-TCP0, α-TCP60, and α-TCP120 cement specimens with and without IP6 surface modification showed mostly α-TCP phase, whereas HAp contents in those cement specimens slightly increased with milling time and were more than those in the starting cement powders. The HAp contents in the α-TCP180 and IP6-α-TCP180 cement specimens were two times more than those in other cement specimens. The HAp contents in the IP6-α-TCP120 and IP6-α-TCP180 cement specimens were significantly more than those in the α-TCP120 and α-TCP180 cement specimens, respectively ($P < 0.05$).

The compressive strength and relative density of the cement specimens fabricated from the α-TCP powders with and without IP6 surface modification were shown in Figure 7. The maximum compressive strength of the IP6-α-TCP cement specimens mostly composed of α-TCP phase was 8.5 ± 1.1 MPa for the IP6-α-TCP120 cement specimen. In contrast, the compressive strength of the α-TCP180 cement specimens composed of α-TCP/HAp biphase was significantly higher (19.0 ± 2.7 MPa) than that of IP6-α-TCP180 cement specimens ($P < 0.05$). No significant difference in the relative density between the α-TCP and IP6-α-TCP cement specimens was confirmed.

Figures 8(a) and 8(e) showing the microstructure of fracture cement provided many voids among the grains in the fracture surface. In Figures 8(b)–8(d) and 8(f)–8(h), small particles packed among the grains were observed, and small particles increased with milling time. No obvious difference in the microstructure of fracture cement between α-TCP and IP6-α-TCP cement specimens was observed.

Next, in order to evaluate the biocompatibility of the cement specimens, we have compared cell proliferation between polystyrene plate and cement specimens (α-TCP120 and IP6-α-TCP120). We have selected the IP6-α-TCP120 cement with the highest compressive strength, and lowest HAp contents among the single-phase α-TCP cements were selected, because that would be expected as the most biodegradable material.

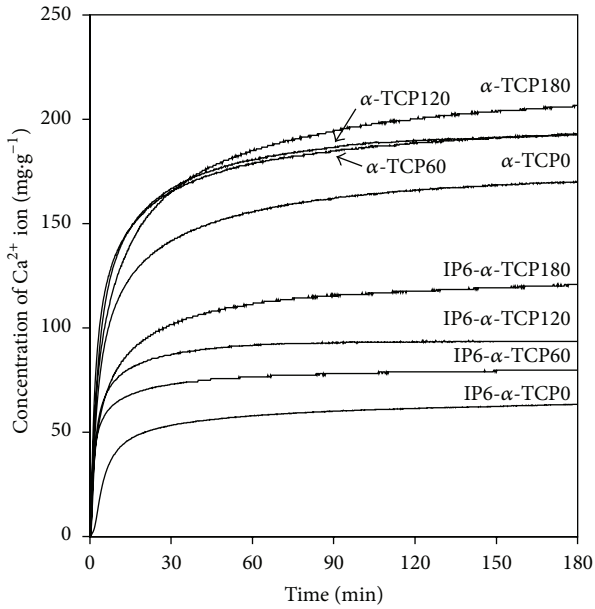

Figure 5: Dissolution of Ca^{2+} ions from the prepared α-TCP powders with and without IP6 surface modification. Dissolution of the IP6-α-TCP powders was lower than that of α-TCP powders without IP6 surface modification.

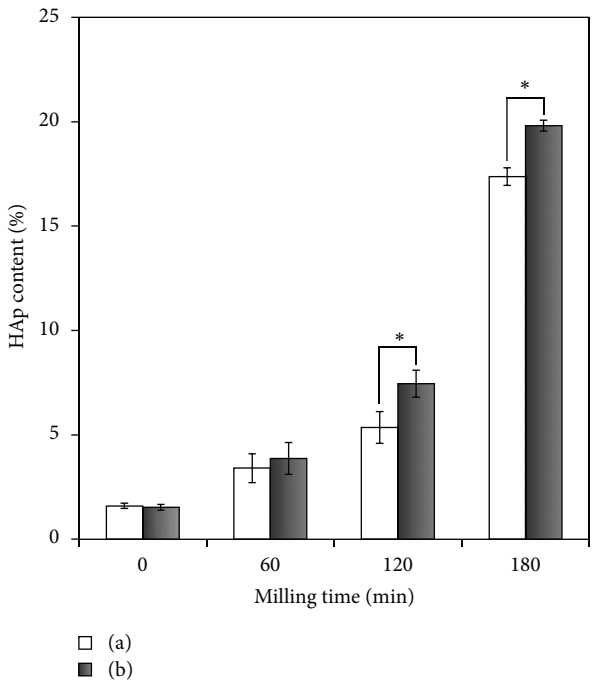

Figure 6: HAp content of the cement specimens after setting for 24 h, fabricated from the α-TCP powders with (a) and without (b) IP6 surface modification at P/L = 1/0.40 [g/cm^3]. Error bars indicated standard error of the mean ($n = 3$). The asterisks (*) showed that $P < 0.05$ by t test. HAp contents in α-TCP0, α-TCP60, and α-TCP120 cement specimens with and without IP6 surface modification slightly increased with milling time and were more than those in the starting cement powders. The HAp contents in the α-TCP180 and IP6-α-TCP180 cement specimens were two times more than those in other cement specimens.

3.3. In Vitro Evaluation of the α-TCP Cement Specimens. Figure 9 showed cell proliferation cocultured with the α-TCP120 and IP6-α-TCP120 cement specimens using Transwell kit. In comparison with cell proliferation of control (polystyrene plate) and α-TCP120 cement, no significant differences between control and α-TCP120 cement was observed. The results suggested that any component from α-TCP120 cement, which affected the cell proliferation, did not release into a medium.

Next, in order to evaluate whether IP6 surface modification affected cell proliferation or not, cell proliferation assay using IP6-α-TCP120 cement was performed. The cell proliferation co-cultured with IP6-α-TCP120 cement was comparable with that of α-TCP120 cement, and no significance in the cell proliferation between α-TCP120 and IP6-α-TCP120 cements was confirmed. This indicated that IP6 surface modification did not have effects on the cell proliferation, and both the α-TCP120 and IP6-α-TCP120 cements were biocompatible materials.

3.4. In Vivo Evaluation of the α-TCP Cement Specimens. As a result of *in vitro* evaluation, no obvious changes in cell proliferation co-cultured with and without cement specimens were seen for each time point (Figure 9). Following the *in vitro* study, *in vivo* biodegradability and biocompatibility of the IP6-α-TCP120 cement specimen were evaluated due to their excellent cell proliferation *in vitro*.

Histological observation of the IP6-α-TCP120 cement specimens after 4, 8, and 24 weeks of implantation was performed using HE (Figures 10(a)–10(f)) and TRAP (Figures 10(g)–10(i)) stainings. Low-magnification images (Figures 10(a)–10(c)) showing the entire cement specimens (C) were not directly in contact with newly-formed bones (N). Figures 10(d)–10(f) showed high-magnification images of the areas indicated by dotted-line squares in Figures 10(a)–10(c), respectively, where the newly formed bones were evident by light pink staining and those increased with milling time at a slight distance from the cement specimens and grew mature at 24 weeks. In the areas of the newly formed bones, aligning osteoblast-like cells (arrows) forming the newly formed osteoids were confirmed in all of the implant periods (Figures 10(d)–10(f)). Meanwhile, TRAP-positive osteoclast-like cells (asterisk) on the surface of the cement specimen resorbing the cement specimens were observed throughout all of the implant periods (Figures 10(g)–10(i)). Rate of resorption, which was calculated from the sectional areas of the cement specimens before and after implantation for 4, 8, and 24 weeks using Figures 10(a)–10(c), was 13.7%, 14.1%, 16.2%, respectively.

4. Discussion

It is well known that α-TCP could be hydrolyzed, resulting in forming a CDHA as indicated by (4) [5, 20, 21] as follows:

$$3Ca_3(PO_4)_2 + H_2O \longrightarrow Ca_9(PO_4)_5(HPO_4)OH \quad (4)$$

The α-TCP was used as a solid component of the CPC because of its high reactivity, and, final product of the CPC

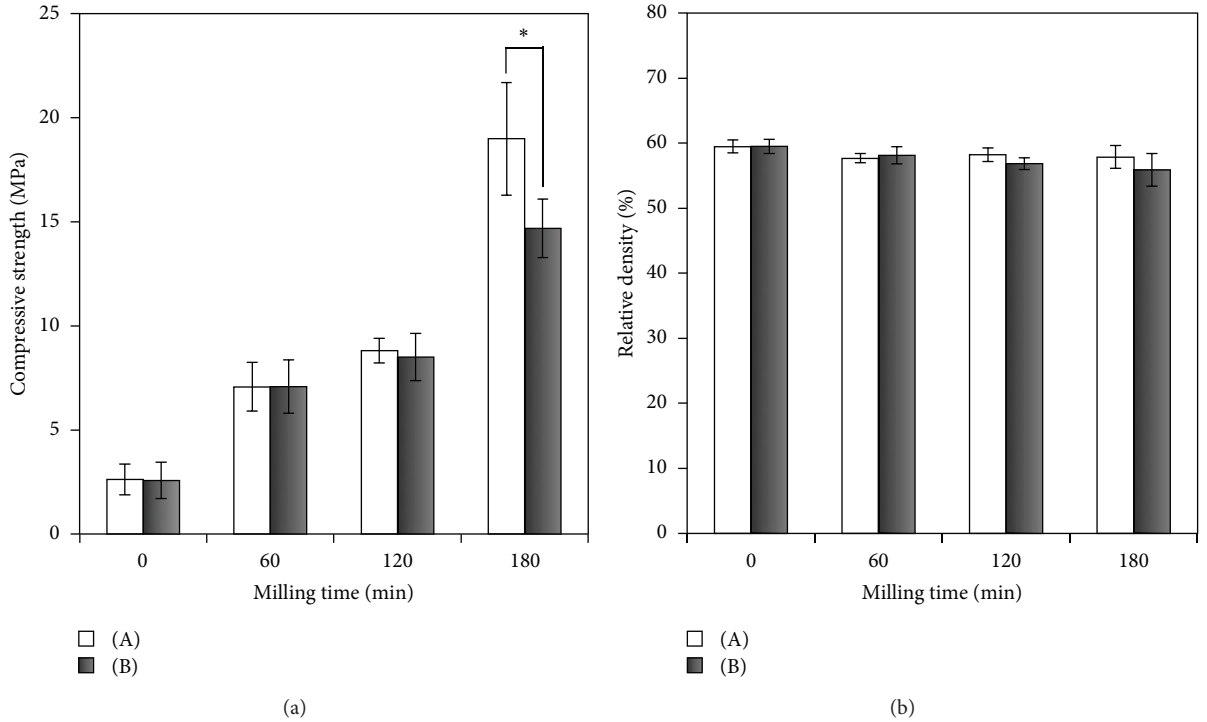

Figure 7: Compressive strength (a) and relative density (b) of the cement specimens after setting for 24 h, fabricated from the α-TCP powders with (A) and without (B) IP6 surface modification at P/L = 1/0.40 [g/cm^3]. Error bars indicated standard error of the mean ($n = 3$). The asterisk (*) showed that $P < 0.05$ by t test. The maximum compressive strength of the IP6-α-TCP cement specimens mostly composed of α-TCP phase was 8.5 ± 1.1 MPa for the IP6-α-TCP120 cement specimen; whereas, the compressive strength of the α-TCP180 cement specimens composed of α-TCP/HAp biphase was the highest (19.0 ± 2.7 MPa).

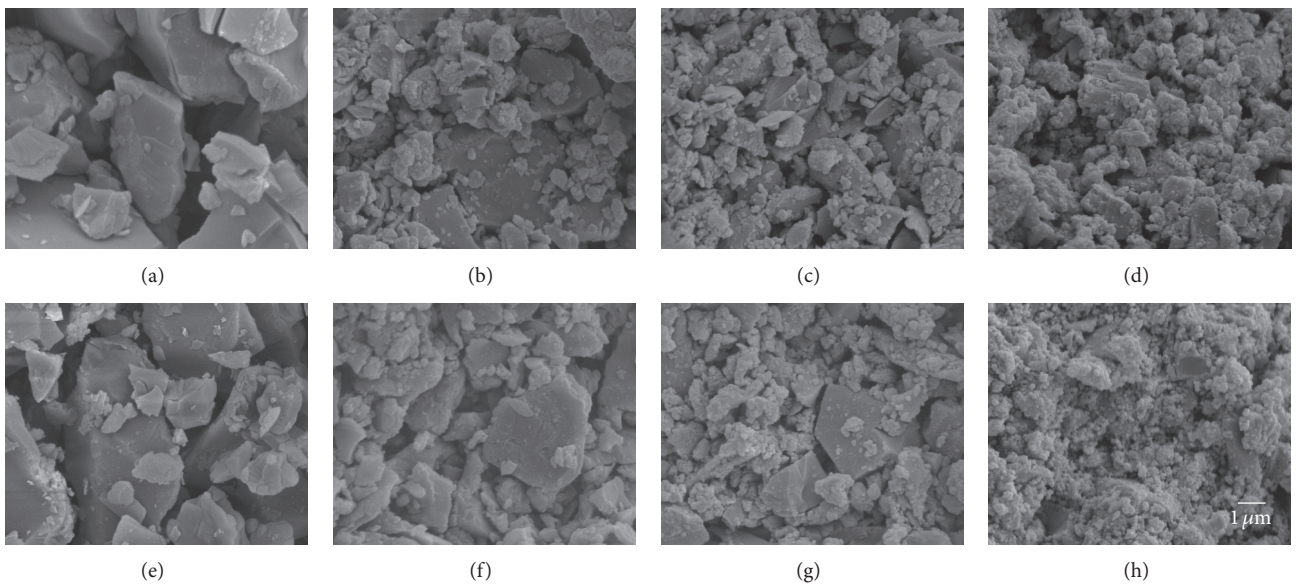

Figure 8: Microstructure of fractured cement surface, fabricated from the α-TCP powders with and without IP6 surface modification at P/L = 1/0.40 [g/cm^3]: (a) α-TCP0, (b) α-TCP60, (c) α-TCP120, (d) α-TCP180, (e) IP6-α-TCP0, (f) IP6-α-TCP60, (g) IP6-α-TCP120, and (h) IP6-α-TCP180. (a) and (e) provided many voids among the grains in the fracture surface. (b)–(d) and (f)–(h) showed small particles packed among the grains, and small particles increasing with milling time.

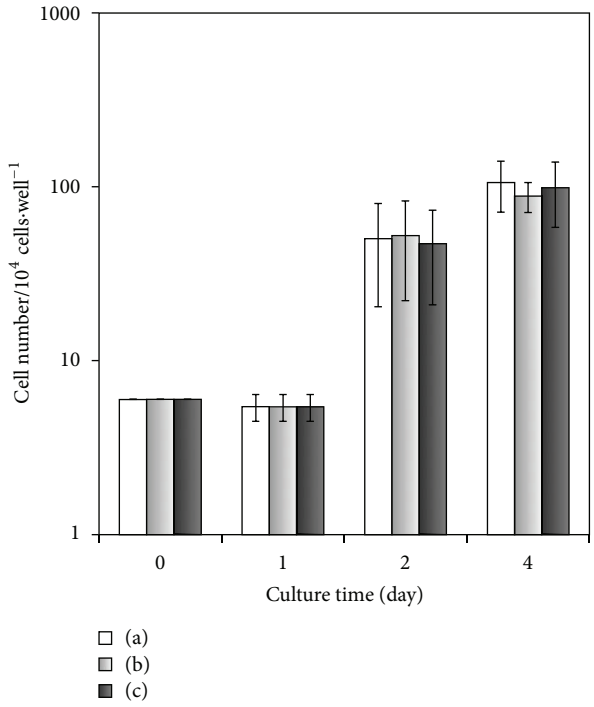

Figure 9: Cell proliferation co-cultured with the α-TCP120 and IP6-α-TCP120 cement specimens using Transwell kit: (a) control (polystyrene plate), (b) α-TCP120 (P/L = 1/0.40 [g/cm^3]), and (c) IP6-α-TCP120 (P/L = 1/0.40). The cement specimens were set on the membrane of Transwell after the cells were cultured for 24 h. Error bars indicated standard error of the mean (n = 3). The cell proliferation of polystyrene plate and two kinds of cement specimen was almost the same level, and no significant differences among them were observed.

was CDHA [22–24]. In order to adjust the particle size of α-TCP as a solid component of the CPC, the α-TCP was mechanically ball milled for appropriate periods [23–27]. Moreover, it was reported that the mechanically ball-milled α-TCP caused decrease in XRD intensities of α-TCP, and led to transformation from crystalline to amorphous state [23–27]. The decrease in XRD intensities and crystallite size of the α-TCP powders was confirmed with increasing of milling time (Figures 1 and 2), implying that the ball milled α-TCP powders contained the amorphous phase in part.

Most of α-TCP phase was maintained up to 120 minutes of milling, and the α-TCP powders over 120 minutes of milling were composed of the both α-TCP and HAp phases (Figure 1). The phase transformation of α-TCP to HAp in milling duration of 120 minutes and longer was due to hydrolysis of the α-TCP during ball-milling, which was evident by the increase in HAp content and specific surface area. In the previous report by Gbureck et al. [23], they showed that prolonged ball-milling of α-TCP did not lead to α-TCP and HAp biphase but amorphous α-TCP in XRD pattern. They used a 99.9% of ethanol as a milling solvent; however, we used pure water as a milling solvent in this paper. Consequently, the α-TCP was hydrolyzed in pure water over 120 minutes of milling.

The particle size of the prepared IP6-α-TCP powders decreased with increasing milling time. As a consequence, the dissolution of the α-TCP powders with and without IP6 surface modification also increased. The results suggested that the decrease in particle size was dominant for dissolution of the α-TCP powders. In addition, IP6 can chelate with Ca^{2+} ions, as previously reported [28, 29]; thus, the adsorption of IP6 on the surface of α-TCP powders may inhibit the dissolution of α-TCP itself. As a result, the dissolution of the IP6-α-TCP powders was lower than that of α-TCP powders without IP6 surface modification, as shown in Figure 5. However, no direct evidence could be obtained that the IP6 was surface modified successfully. Because of low IP6 concentration used in this paper (1000 ppm), it was not detected by Fourier transform infrared spectroscopic analysis. Therefore, further analysis will be necessary for detection of IP6 on the surface of α-TCP.

The α-TCP cement based on chelating mechanism of IP6 was developed for the first time in this paper. The compressive strength of the α-TCP cement specimens with and without IP6 surface modification increased with milling time; however, the relative density of these cement specimens did not change and HAp contents of these cement specimens, excluding α-TCP180 and IP6-α-TCP180, also did not change compared to those of the cement powders. Increase in compressive strength of the α-TCP cement specimens was due to decrease in particle size of α-TCP powders, which was evident by increase in packing degree of the α-TCP powders in Figure 8. However, difference in the relative density of the cement specimens was not observed because of small change in the compressive strength. Furthermore, the cement specimens were fabricated with high P/L ratio (1/0.40 [g/cm^3]) and the α-TCP powders were barely hydrolyzed during setting of the cements; therefore, no change in HAp contents of α-TCP cement specimens, except for α-TCP180 and IP6-α-TCP180, was observed. Significances in the HAp contents between α-TCP120 and IP6-α-TCP120 and α-TCP180 and IP6-α-TCP180 were because of the higher HAp contents in the IP6-α-TCP120 and IP6-α-TCP180 powders than those of the α-TCP120 and α-TCP180 powders as shown in Figure 2. The HAp contents in α-TCP180 and IP6-α-TCP180 cement specimens were more than those of other cement specimens, and the compressive strength of the α-TCP180 cement specimen was significantly more than that of α-TCP180 cement specimen. The results indicated that the α-TCP180 and IP6-α-TCP180 powders were slightly hydrolyzed during setting of the cements. As a consequence, enhancement in compressive strength of these two cement specimens was not presumably caused by only increase in HAp contents but also entanglement of each particle and chelate-bonding of IP6. However, obvious needle-shaped or plate-shaped crystals formed by hydrolysis of the α-TCP, as reported by TenHuisen and Brown [21] and Ginebra et al. [22], were not observed in the microstructures (Figure 8).

Regarding *in vitro* evaluation of HAp cements, we have previously elucidated that IP6 surface modification of the HAp particles with 1000 ppm IP6 did not affect the biocompatibility of the cement specimen *in vitro* [8, 11]. The present cell-culture test using Transwell kit (Figure 9) indicated that

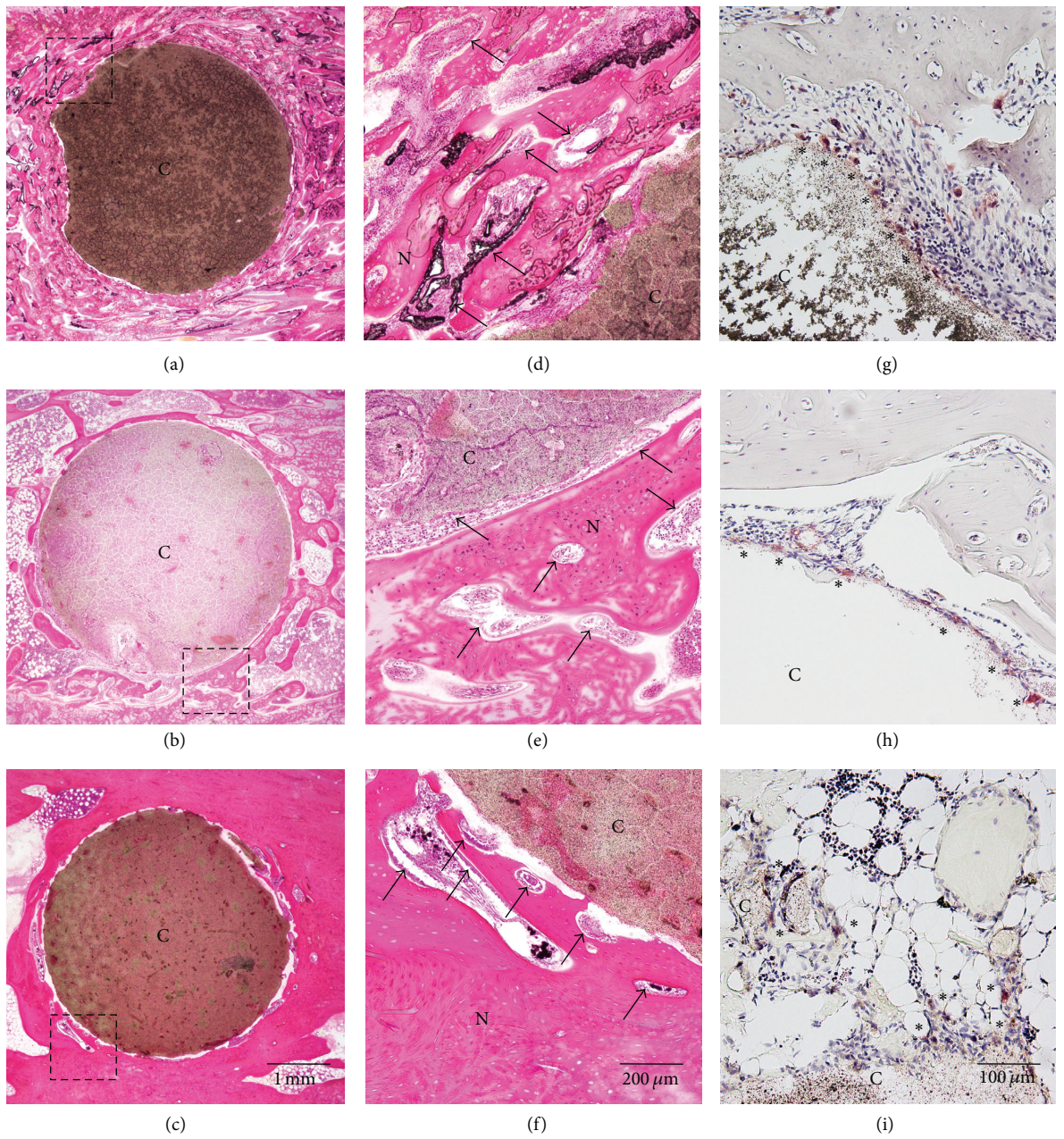

FIGURE 10: Histological sections showing IP6-α-TCP120 (P/L = 1/0.40 [g/cm^3]) cement specimens implanted into the rabbit tibia. (a)–(f): undecalcified sections stained with HE; (g)–(i): decalcified sections stained with TRAP. (a), (d), and (g): 4 weeks of implantation; (b), (e), and (h): 8 weeks of implantation; (c), (f), and (i): 24 weeks of implantation. The low-magnification images (a)–(c) showed the entire cement specimen (C), and (d)–(f) presented high-magnification images of the dotted square areas shown in (a)–(c), respectively, where the newly formed bones were evident by light pink staining. The arrows in (d)–(f) indicated aligning osteoblast-like cells forming the newly formed bones (N). The asterisks (*) in (g)–(i) represented TRAP-positive osteoclast-like cells resorbing the cement.

there was no significance in cell proliferation between α-TCP cements with and without IP6 surface modification, and both α-TCP cements did not affect the biocompatibility.

In vivo studies indicated that the newly formed bones increased with milling time at a slight distance from the cement specimens and grew mature at 24 weeks (Figures 10(d)–10(f)). The surface of the IP6-α-TCP120 cement specimens was resorbed by TRAP-positive osteoclast-like cells (Figures 10(g)–10(i)) throughout all of the implant periods.

The biological behavior of α-TCP has previously been studied in several *in vivo* studies [19, 30–34]; however, no report existed about α-TCP-based cement composed of α-TCP phase, because α-TCP was used as the solid component of hydraulic CPC [5, 17, 18]. Kihara et al. [33] reported that, in the implantation of α-TCP particles (~300 μm diameter) into cranial bone defects in rabbits, a "reticulate structure" was developed among the α-TCP particles after 1 week as a consequence of the degradation of α-TCP, and newly formed

bone was observed after 8 weeks. Yamada et al. [19] conducted a histological and histomorphometrical study of porous α-TCP blocks as bone graft material for augmenting alveolar ridges. The α-TCP block notably started degrading after 4 weeks, and was severely degraded after 8 weeks. Residual α-TCP particles surrounded by newly formed bone decreased over time, and both particles and newly formed bone were simultaneously resorbed by osteoclast-like cells. Both reports suggested that the α-TCP ceramics were potential biodegradable material. In this paper, the resorption of the cement specimens by osteoclast-like cells was observed throughout all of the implant periods; however, most of the cements (83.8%) remained even after 24 weeks of implantation. Oonishi et al. reported that α-TCP granules with 300 μm in diameter were mostly resorbed after 12 weeks of implantation in the rabbit model [31]. The present IP6-α-TCP120 cements were relatively dense (56.8 ± 0.9% of relative density) with no interconnected pores in the cement, and they could be resorbed chemically and biologically only from the surface of the cement. Thus, the resorption rate of the IP6-α-TCP cement was slow. Furthermore, less dissolution of the IP6-α-TCP120 powder than that of the α-TCP120 powder as shown in Figure 5 suggested that the IP6-α-TCP120 cement was less soluble than the α-TCP120 cement. Therefore, long-term studies will be necessary to evaluate the complete degradability of the cement.

5. Conclusions

The single-phase α-TCP powder for fabrication of IP6-α-TCP cement was obtained by ball milling of α-TCP for 120 min. The resulting cement, which was fabricated by mixing the IP6-α-TCP120 and pure water, was mostly composed of α-TCP phase, and the compressive strength of the cement was 8.5 ± 1.1 MPa, which suggested that the cements set with keeping the crystallite phase of starting cement powder. The enhancement in the compressive strength with milling time was achieved by a decrease in particle size of the cement powders. *In vitro* cell-culture test indicated biocompatibility of the cement. *In vivo* studies showed that the newly formed bones increased with milling time at a slight distance from the cement specimens and grew mature at 24 weeks, and the surface of the cement was resorbed by TRAP-positive osteoclast-like cells up till 24 weeks of implantation. The present IP6-α-TCP cement with biodegradability and biocompatibility is a promising candidate for application as a novel paste-like artificial bone.

Conflict of Interests

None of the authors have any conflict of interests associated with this paper.

References

[1] K. Ishikawa, S. Takagi, L. C. Chow, and Y. Ishikawa, "Properties and mechanisms of fast-setting calcium phosphate cements," *Journal of Materials Science*, vol. 6, no. 9, pp. 528–533, 1995.

[2] U. Gbureck, J. E. Barralet, K. Spatz, L. M. Grover, and R. Thull, "Ionic modification of calcium phosphate cement viscosity. Part I: hypodermic injection and strength improvement of apatite cement," *Biomaterials*, vol. 25, no. 11, pp. 2187–2195, 2004.

[3] J. E. Barralet, M. Tremayne, K. J. Lilley, and U. Gbureck, "Modification of calcium phosphate cement with α-hydroxy acids and their salts," *Chemistry of Materials*, vol. 17, no. 6, pp. 1313–1319, 2005.

[4] Y. Miyamoto, K. Ishikawa, M. Takechi et al., "Histological and compositional evaluations of three types of calcium phosphate cements when implanted in subcutaneous tissue immediately after mixing," *Journal of Biomedical Materials Research A*, vol. 48, pp. 36–42, 1999.

[5] H. Monma and T. Kanazawa, "The hydration of α-tricalcium phosphate," *Yogyo-Kyokai-Shi*, vol. 84, pp. 209–213, 1976.

[6] W. E. Brown and L. C. Chow, "Dental restorative cement pastes," US Patent No. US4518430, 1985.

[7] D. Apelt, F. Theiss, A. O. El-Warrak et al., "*In vivo* behavior of three different injectable hydraulic calcium phosphate cements," *Biomaterials*, vol. 25, no. 7-8, pp. 1439–1451, 2004.

[8] M. Aizawa, Y. Haruta, and I. Okada, "Development of novel cement processing using hydroxyapatite particles modified with inositol phosphate," in *Archives of BioCeramics Research*, vol. 3, pp. 134–138, 2003.

[9] Y. Horiguchi, A. Yoshikawa, K. Oribe, and M. Aizawa, "Fabrication of chelate-setting hydroxyapatite cements from four kinds of commercially-available powder with various shape and crystallinity and their mechanical property," *Nippon Seramikkusu Kyokai Gakujutsu Ronbunshi*, vol. 116, no. 1349, pp. 50–55, 2008.

[10] T. Konishi, Z. Zhuang, M. Mizumoto, M. Honda, and M. Aizawa, "Fabrication of chelate-setting cement from hydroxyapatite powder prepared by simultaneously grinding and surface-modifying with sodium inositol hexaphosphate and their material properties," *Journal of the Ceramic Society of Japan*, vol. 120, pp. 1–7, 2012.

[11] T. Konishi, Y. Horiguchi, M. Mizumoto et al., "Novel chelate-setting calcium-phosphate cements fabricated with wet-synthesized hydroxyapatite powder," *Journal of Materials Science*, vol. 24, pp. 611–621, 2013.

[12] T. H. Dao, "Polyvalent cation effects on myo-inositol hexakis dihydrogenphosphate enzymatic dephosphorylation in dairy wastewater," *Journal of Environmental Quality*, vol. 32, no. 2, pp. 694–701, 2003.

[13] C. J. Martin and W. J. Evans, "Phytic acid-metal ion interactions. II. The effect of pH on Ca(II) binding," *Journal of Inorganic Biochemistry*, pp. 2717–2730, 1986.

[14] S. Takahashi, T. Konishi, K. Nishiyama et al., "Fabrication of novel bioresorbable β-tricalcium phosphate cement on the basis of chelate-setting mechanism of inositol phosphate and its evaluation," *Nippon Seramikkusu Kyokai Gakujutsu Ronbunshi/Journal of the Ceramic Society of Japan*, vol. 119, no. 1385, pp. 35–42, 2011.

[15] T. Konishi, S. Takahashi, M. Mizumoto, M. Honda, K. Oribe, and M. Aizawa, "Effect of the addition of various polysaccharides on the material properties and cytotoxicity of chelate-setting β-tricalcium phosphate cement," *Phosphorus Research Bulletin*, vol. 26, pp. 59–64, 2012.

[16] T. Konishi, S. Takahashi, and Z. Zetal, "Biodegradable β-tricalcium phosphate cement with anti-washout property based on chelate-setting mechanism of inositol phosphate," *Journal of Materials Science*, 2013.

[17] F. H. Lin, C. J. Liao, K. S. Chen, J. S. Sun, and C. P. Lin, "Petal-like apatite formed on the surface of tricalcium phosphate ceramic after soaking in distilled water," *Biomaterials*, vol. 22, no. 22, pp. 2981–2992, 2001.

[18] P. Ducheyne, S. Radin, and L. King, "The effect of calcium phosphate ceramic composition and structure on in vitro behavior. I. Dissolution," *Journal of Biomedical Materials Research*, vol. 27, no. 1, pp. 25–34, 1993.

[19] M. Yamada, M. Shiota, Y. Yamashita, and S. Kasugai, "Histological and histomorphometrical comparative study of the degradation and osteoconductive characteristics of α- and β-tricalcium phosphate in block grafts," *Journal of Biomedical Materials Research B*, vol. 82, no. 1, pp. 139–148, 2007.

[20] Y. Li, X. Zhang, and K. de Groot, "Hydrolysis and phase transition of alpha-tricalcium phosphate," *Biomaterials*, vol. 18, no. 10, pp. 737–741, 1997.

[21] K. S. TenHuisen and P. W. Brown, "Formation of calcium-deficient hydroxyapatite from α-tricalcium phosphate," *Biomaterials*, vol. 19, no. 23, pp. 2209–2217, 1998.

[22] M. P. Ginebra, E. Fernandez, F. C. M. Driessens et al., "The effects of temperature on the behaviour of an apatitic calcium phosphate cement," *Journal of Materials Science*, vol. 6, no. 12, pp. 857–860, 1995.

[23] U. Gbureck, J. E. Barralet, L. Radu, H. G. Klinger, and R. Thull, "Amorphous α-tricalcium phosphate: preparation and aqueous setting reaction," *Journal of the American Ceramic Society*, vol. 87, no. 6, pp. 1126–1132, 2004.

[24] C. L. Camiré, P. Nevsten, L. Lidgren, and I. McCarthy, "The effect of crystallinity on strength development ofα-TCP bone substitutes," *Journal of Biomedical Materials Research B*, vol. 79, pp. 159–165, 2006.

[25] C. L. Camiré, U. Gbureck, W. Hirsiger, and M. Bohner, "Correlating crystallinity and reactivity in an α-tricalcium phosphate," *Biomaterials*, vol. 26, no. 16, pp. 2787–2794, 2005.

[26] M. Bohner, A. K. Malsy, C. L. Camiré, and U. Gbureck, "Combining particle size distribution and isothermal calorimetry data to determine the reaction kinetics of α-tricalcium phosphate-water mixtures," *Acta Biomaterialia*, vol. 2, no. 3, pp. 343–348, 2006.

[27] T. J. Brunner, R. N. Grass, M. Bohner, and W. J. Stark, "Effect of particle size, crystal phase and crystallinity on the reactivity of tricalcium phosphate cements for bone reconstruction," *Journal of Materials Chemistry*, vol. 17, no. 38, pp. 4072–4078, 2007.

[28] C. J. Martin and W. J. Evans, "Phytic acid-metal ion interactions. II. The effect of pH on Ca(II) binding," *Journal of Inorganic Biochemistry*, vol. 27, pp. 17–30, 1986.

[29] B. M. Luttrell, "The biological relevance of the binding of calcium ions by inositol phosphates," *Journal of Biological Chemistry*, vol. 268, no. 3, pp. 1521–1524, 1993.

[30] K. Ikami, M. Iwaku, and H. Ozawa, "An ultrastructural study of the process of hard tissue formation in amputated dental pulp dressed with α-tricalcium phosphate," *Archives of Histology and Cytology*, vol. 53, no. 2, pp. 227–243, 1990.

[31] H. Oonishi, L. L. Hench, J. Wilson et al., "Comparative bone growth behavior in granules of bioceramic materials of various sizes," *Journal of Biomedical Materials Research*, vol. 44, no. 1, pp. 31–43, 1999.

[32] M. Kitamura, C. Ohtsuki, H. Iwasaki, S. I. Ogata, M. Tanihara, and T. Miyazaki, "The controlled resorption of porous α-tricalcium phosphate using a hydroxypropylcellulose coating," *Journal of Materials Science*, vol. 15, no. 10, pp. 1153–1158, 2004.

[33] H. Kihara, M. Shiota, Y. Yamashita, and S. Kasugai, "Biodegradation process of α-TCP particles and new bone formation in a rabbit cranial defect model," *Journal of Biomedical Materials Research B*, vol. 79, no. 2, pp. 284–291, 2006.

[34] M. Nyan, D. Sato, H. Kihara, T. MacHida, K. Ohya, and S. Kasugai, "Effects of the combination with α-tricalcium phosphate and simvastatin on bone regeneration," *Clinical Oral Implants Research*, vol. 20, no. 3, pp. 280–287, 2009.